This is a repository copy of *Thermoluminescence measurements of trap depth in alkali feldspars extracted from bedrock samples*.

White Rose Research Online URL for this paper:
http://eprints.whiterose.ac.uk/109867/

Version: Accepted Version

Article:

Brown, N.D. and Rhodes, E.J. (2017) Thermoluminescence measurements of trap depth in alkali feldspars extracted from bedrock samples. Radiation Measurements, 96. pp. 53-61. ISSN 1350-4487

https://doi.org/10.1016/j.radmeas.2016.11.011

Reuse

Unless indicated otherwise, fulltext items are protected by copyright with all rights reserved. The copyright exception in section 29 of the Copyright, Designs and Patents Act 1988 allows the making of a single copy solely for the purpose of non-commercial research or private study within the limits of fair dealing. The publisher or other rights-holder may allow further reproduction and re-use of this version - refer to the White Rose Research Online record for this item. Where records identify the publisher as the copyright holder, users can verify any specific terms of use on the publisher's website.

Takedown

If you consider content in White Rose Research Online to be in breach of UK law, please notify us by emailing eprints@whiterose.ac.uk including the URL of the record and the reason for the withdrawal request.

eprints@whiterose.ac.uk
https://eprints.whiterose.ac.uk/

Thermoluminescence measurements of trap depth in alkali feldspars extracted from bedrock samples

N.D. Brown[a,*], E.J. Rhodes[a,b]

[a] *Department of Earth, Planetary, and Space Sciences, University of California, Los Angeles, 595 Charles Young Drive East, Box 951567, Los Angeles, CA 90095-1567, USA*
[b] *Department of Geography, Winter Street, University of Sheffield, Sheffield, South Yorkshire S10 2TN, UK*
Authors' manuscript of a paper published in Radiation Measurements 96, 53-61, http://dx.doi.org/10.1016/j.radmeas.2016.11.011

Abstract

Various measurements of thermal trap depth are evaluated for K-feldspar grains extracted from a bedrock sample. The initial rise method and the various heating rates method yield consistent results for both the natural signal ($E = 1.23$ and 1.16 eV, respectively) and for a regenerative dose of 64 Gy (0.83 and 0.78 eV). For the fractional glow curve, apparent E-values range from 0.39 eV to a plateau around 1.50 eV. The highest values for the natural and regenerative signals are obtained using the newly-developed post-isothermal TL (pI-TL) method wherein the isothermal loss curves (gotten by subtracting TL curves obtained after different preheat durations) are fitted in the initial rise region on an Arrhenius plot. For a dose of 12.8 Gy, this method measures apparent E-values ranging from 0.73 eV to a plateau near 1.84 ± 0.06 eV. We repeat this analysis on three additional feldspar samples (two perthites and a high albite) to get a mean value of $E = 1.86 \pm 0.03$ eV. The same analysis of natural aliquots of the K-feldspar sample yields similar results, with the two highest E-values at 1.81 and 1.86 eV. The kinetic order does not systematically vary with isothermal holding temperature or duration but remains relatively constant at 1.6 ± 0.3 (regenerative dose) and 1.5 ± 0.5 (natural dose). The apparent frequency factor, measured assuming a single E-value of 1.86 eV, decreases systematically ($\sim 10^{23} - 10^{12}\ s^{-1}$) with hold temperature and duration, a result which is consistent with a thermally-activated, distance-dependent tunneling model for feldspar thermoluminescence (i.e., a single trap depth and a continuum of apparent frequency factors). Frequency factor values measured following identical isothermal treatments are comparable between the natural and regenerative post-isothermal TL curves. By contrast, if different E-values are assumed, the apparent frequency factor values appear stochastic. Finally, it is speculated that the plateau of pI-TL E-values may be interpreted as the thermal depth of the main dosimetric trap measured with IRSL protocols.

Keywords: feldspar thermoluminescence, fractional glow curve, feldspar trap depth, post-isothermal TL

---

*Corresponding author
Email addresses: nathan.david.brown@ucla.edu (N.D. Brown), ed.rhodes@sheffield.ac.uk (E.J. Rhodes)

1. Introduction

One critical parameter in understanding how the feldspar luminescence system will evolve in different thermal scenarios is the thermal activation energy required for recombination (E-value). A number of measurements can be used to constrain this parameter under first-order kinetics; however, in the case of feldspar luminescence, which exhibits a continuum of thermoluminescence (TL) signals (Grün and Packman, 1994; Visocekas et al., 1996) and is generally considered to exhibit non-first-order recombination kinetics (Ankjaergaard et al., 2006; Jain and Ankjaergaard, 2011), the determination of this parameter is not straightforward, nor is it necessarily a single trap being accessed during a TL measurement (Balescu and Lamothe, 1992; Murray et al., 2009).

The basic obstacle that must be overcome in order to measure the E-values of a sample, is that TL glow curves (following natural or laboratory irradiations) comprise overlapping emissions of different stability. For potassium-rich feldspars, this is complicated by the presence of a second TL peak at higher temperatures (centered around 330 °C for $\beta = 5$ °C/s), such that the measured glow curve contains a broad, asymmetric peak at lower temperatures (apex near 100 °C), and a high-temperature peak (or two peaks; e.g., Murray et al., 2009), often embedded within the first (Duller, 1997). This range of stability in the broad, lower-temperature emission has been interpreted as representing multiple, discrete trap depths (Strickertsson, 1985; Kirsh et al., 1987) or a continuum of trap depths (Sanderson, 1988). Alternately, a continuum of recombination distances may produce this behavior (Jain et al., 2012). Pagonis et al. (2014) recently concluded that either mechanism could produce the observed TL data. Regardless, to measure the kinetic properties for a portion of a feldspar TL glow curve (e.g., a single trap depth or a limited range of recombination distances), one must isolate that particular emission, either experimentally or mathematically.

To determine the thermal trap depths of the dosimetric traps producing the TL or IRSL signals, workers have relied chiefly upon: the initial rise method (hereafter, IRM), usually in conjunction with the fractional glow curve method (hereafter, FGC; Strickertsson, 1985; Visocekas et al., 1996; Chruścińska, 2001); isothermal loss measurements (Sanderson, 1988; Guralnik et al., 2015); and curve fitting methods (Pagonis et al., 2014; Jain et al., 2015) (for a full discussion of conventional methods, see pp. 101 - 130 of Chen and McKeever, 1997). The following incomplete list of the resulting E-values can be broadly categorized as either singular, continuous, or multiple and discrete. The singular estimates for the IRSL source trap include >1.5 (Jain and Ankjaergaard, 2011), 1.66 (Li and Tso, 1997), 1.72 (Li et al., 1997), 1.71 ± 0.08 (Murray et al., 2009), 1.92 - 2.06 (Li and Li, 2013), and ∼2 (Jain et al., 2015) eV. Pagonis et al. (2014) estimated a continuum of depths from 1.1 to 1.8 eV in plagioclase; Strickertsson (1985) assumed first-order kinetics to fit six TL peaks between 0.76 and 1.80 eV; and Kirsh et al. (1987) estimated five distinct peaks, ranging from 0.70 to 1.39 eV.

In this study, we estimate the apparent thermal activation energies responsible for natural and laboratory TL signals in feldspar crystals extracted from bedrock samples. First, we apply the initial rise method, the various heating rates method, and the fractional glow curve technique. Second, we develop a new E-value estimation technique based on the isothermal decay of TL curves: the post-isothermal TL (pI-TL) method. This method quantifies (by glow curve subtraction) the loss between hold times at various temperatures. By doing so, we quantify not only the magnitude of isothermal decay but also the shape of the TL signal that would have resulted during thermal stimulation. In other words, those emissions which are of lesser stability are stripped away, allowing for peak shape analysis of a narrow range of thermal stabilities. Finally, the pI-TL results are discussed in terms of recombination kinetics, including the variation in kinetic order and frequency factor.

2. Samples and methodology

2.1. Sample collection

Bedrock samples were collected from two locations. Sample J0165 is a granodiorite taken from a vertical transect of the Yucaipa Ridge block, a fault-bounded, tectonic block within the San Bernardino Mountains in southern California (Spotila et al., 1998). Samples J0995 (quartzofeldspathic gneiss), J0999 (granite), and J1001 (granite) were collected from a glacial valley within the Beartooth uplift, a 60 $\times$ 125 km block of Precambrian crystalline basement initially exhumed during the Laramide Orogeny (Wise, 2000). Samples were collected by detaching chunks of *in situ* bedrock by hammer and chisel.

2.2. Sample preparation and luminescence instrumentation

Samples were first spray-painted with a contrasting color. They were then broken into smaller fragments under dim, amber LED lighting. The light-exposed, outer-surface pieces (as identified by the presence of spray-paint) were discarded and the unexposed inner pieces were gently ground using a pestle and mortar. The feldspar grains of 175-400 μm were then isolated from the rubble. Subsamples were wet-sieved, treated with 3% HCl, separated by density using lithium metatungstate (ρ <2.565 g/cm^3; Rhodes 2015), and treated with 10% HF for 10 minutes to remove the outer layer from the grains and thereby enhance the sample brightness. Grains were mounted on stainless steel discs in a small-diameter (ca. 3-5 mm) monolayer using silicone oil.

Luminescence measurements were carried out using a TL-DA-20 Risø automated reader equipped with a ^{90}Sr/^{90}Y beta source (Bøtter-Jensen et al., 2003). TL emissions were detected through a Schott BG3-BG39 filter combination in a nitrogen atmosphere. Unless otherwise noted, TL glow curves were measured at a heating rate of 5 °C/s.

2.3. Sample compositions

Several separated grains of each sample were prepared for electron-probe microanalysis (EPMA) to determine their chemical compositions. These grains were mounted within epoxy, the surface of which was then progressively polished to expose the internal surfaces of grains. Prior to analysis, this mount was coated with a surficial layer of carbon to avoid electrical charging during electron bombardment.

Table 1: Composition of feldspar samples, as determined by electron-probe microanalysis.

		Endmember composition			Elemental composition		
Sample	n	An (mol%)	Ab (mol%)	Or (mol%)	Ca (wt%)	Na (wt%)	K (wt%)
J0165	4	0.3	10.5	89.3	0.0	0.9	12.8
J00995	4	0.1	99.6	0.3	0.0	8.9	0.0
J0999							
Na-rich zones	3	18.5	78.5	3.0	2.8	6.8	0.4
K-rich zones	2	0.0	3.6	96.3	0.0	0.3	13.7
J1001							
Na-rich zones	3	8.0	90.3	1.7	1.3	8.1	0.3
K-rich zones	3	0.1	3.8	96.2	0.0	0.3	13.9

The mounted and polished grains were then measured with a JEOL JXA-8200 electron-probe microanalyzer. First, backscattered electron (BSE) images were acquired to assess the compositional structure of grains, and then spot analyses with wavelength-dispersive spectroscopy (WDS) were used to quantitatively determine the K, Na, and Ca abundances of each grain (Huot and Lamothe, 2012). Grains with more heterogeneous compositions (i.e., phases of disparate average Z-values) were measured multiple times to quantify each phase. Duplicate measurements were performed to assess reproducibility. Spot analyses were performed using a defocused electron beam of diameter 10 μm, an accelerating voltage of 15 keV, and a beam current of 15 nA. Immediately prior to measurement, spectrometer calibration was performed with anorthite, albite, and K-feldspar standards. Spot analyses were rejected when the interpreted total mass was outside the range of 98 - 102%.

The compositions of all samples are listed in Table 1. The analyzed grains of J0165 are K-feldspars, with an average composition of Or_{89}. Sample J0995 is high albite, $An_{0.1}$. Samples J0999 and J1001 both exhibit perthitic textures. In sample J0999, zones alternate between average compositions of An_{25} and Or_{96} and J1001 alternates between An_8 and Or_{96}.

3. Determining thermal trap depths in K-feldspar

The terms used throughout this study are described in Table 2.

3.1. Initial rise method

The initial rise method (IRM) plots the natural log of the normalized TL intensity as a function of the inverse temperature, analogous to an Arrhenius plot. If the concentrations of trapped electrons and recombination centers are effectively constant (a reasonable assumption for the low-temperature region of a stimulation curve), then the TL intensity with temperature should go as:

$$I(T) \propto \exp\big(-E/k_B T\big), \tag{1}$$

Table 2: Nomenclature used in this study.

Term	Description
E	Thermal trap depth
s	Frequency factor
b	Kinetic order
k_B	Boltzmann constant (8.617×10^{-5} eV $\cdot$ K^{-1})
T_m	Temperature at maximum intensity
$T_{1/2}$	Temperature at half-maximum intensity
β	Heating rate
IRM	Initial rise method
VHRM	Various heating rates method
FGC	Fractional glow curve
pI-TL	Post-isothermal TL

which implies that a straight line fitted to $\ln(I(T))$ plotted against $1/T$ should have a slope of $-E/k_B$ (Chen and Kirsh, 1981, p.148). The results of the IRM are shown for K-feldspar extract of Yucaipa Ridge bedrock sample J0165, for the natural luminescence signal (Fig. 1(a)) and following a laboratory beta dose of 64 Gy (Fig. 1(b))(see the Supplementary Materials for the original TL measurements). A heating rate of 0.1 °C/s was used to minimize errors associated with thermal lag. Three aliquots were used in both cases and remarkable inter-aliquot consistency was found. The apparent activation energies of the natural (1.23 eV) and regenerative (0.83 eV) signals differ substantially, with the E-value following 64 Gy being far too shallow to retain electrons for longer than a few days at room temperature.

3.2. Various heating rates method

The various heating rates method (VHRM) exploits the fact that the temperature of maximum TL emission intensity (T_m) can be expressed in terms of the heating rate, β:

$$\beta = (sk_B/E)T_m^2 \exp\big(-E/k_BT_m\big), \tag{2}$$

so that the plot of $\ln(T_m^2/\beta)$ versus $(1/T_m)$ can be fitted with a straight line of slope $-E/k_B$. To measure the apparent trap depth of the natural signal, three aliquots were heated for each heating-rate: 0.1, 0.5, 1, 5, and 10 °C/s. For the apparent E value after 64 Gy, the same 3 aliquots were heated at 0.1, 0.3, 1, 3, and 10 °C/s. The resulting E values of 1.16 and 0.78 eV are shown for the natural (Fig. 1(c)) and regenerative (Fig. 1(d)) signals (see the Supplementary Materials for the original TL measurements).

3.3. Fractional glow curve analysis

To probe multiple traps of similar depths (e.g., a continuum of depths or tunneling distances), researchers have developed the fractional glow curve (FGC) (Rudlof et al., 1978; Kirsh et al., 1987), which involves a series of preheats to progressively higher temperatures. After holding at a given temperature, the sample is cooled before heating to a slightly higher hold temperature and so on. In this way, the lowest temperature region is investigated (and thereby emptied) before the next-highest temperature region is investigated, thereby minimizing overlap from the lower-temperature region.

Although recent feldspar models (Poolton et al., 1995; Jain and Ankjaergaard, 2011) do not require a distribution of trap depths, the distribution in sub-conduction-band recombination distances should result in a similar effect of overlapping TL peaks (Jain et al., 2012). Therefore, the FGC for a single aliquot of J0165 was measured by first administering a dose of 12.8 Gy, then heating the sample at 5 °C/s to a hold temperature of T °C for 100 s, with T ranging from 20 to 500 °C in increments of 20 °C (Fig. 2(a)). Unfortunately, at $T > 320\ °C$, the signal intensity was similar in magnitude to the thermal background, precluding analysis beyond this point. The initial rise regions of the individual heating steps following a single beta dose of 64 Gy (Fig. 2(a)) were then fitted with a straight line having a slope of $-E/k_B$ (see Section 3.1). These E-values are plotted against the corresponding hold temperature (Fig. 2(b); cf. Fig. 3.14 of Chen and McKeever, 1997).

Two observations can be made about Fig. 2(b). First, a relationship seems to exist between the final temperature and the E-value, representing a gradation in apparent site stability, perhaps due to increasing recombination distances (if the E-values are artifacts), or perhaps deeper traps are progressively accessed (if the E-values are real). Second, this linear increase in FGC E-values (0.97 - 1.51 eV) extends past the trap depth of the natural TL signal as calculated with the IRM and VHRM results (1.23 and 1.16 eV, respectively) (Fig. 1(a) and (c)).

3.4. Post-isothermal TL (pI-TL) curve analysis

An alternate approach is to monitor how the TL shape changes following isothermal treatments of various durations. For analysis of the regenerative signal, the same aliquot of sample J0165 was repeatedly given the same dose of 12.8 Gy and then held at T °C for t s, where T ranged from 100 to 350 °C in increments of 50 °C, and t = 0, 3, 10, 30, 100, 300, 1000 s. Following each isothermal treatment, the aliquot was cooled to room temperature before a TL measurement at 5 °C/s to 500 °C. These TL curves are shown with linear and logarithmic y-axes (Fig. 3(a) and inset, respectively). The advantage of this approach is based upon the ability to isolate the luminescence emitted during hold-times by subtracting one TL curve from another. In other words, each subtracted curve represents the pseudo-TL curve that would be depleted during that isothermal treatment. Fig. 3(b) shows the regenerative TL lost during the hold time of t = 3-10 s, 10-30 s, and so on, for all the hold temperatures.

For analysis of the post-isothermal TL natural signals, a multi-aliquot approach is necessary, where each heat treatment is performed on a different unbleached natural aliquot of sample J0165 (Fig.4(a)). The TL emissions of each aliquot were normalized to a subsequent test dose response (maximum TL intensity following a dose of 1.3 Gy). Because the natural glow curve is not significantly eroded by the lower temperature treatments, the isothermal treatments of the natural signals were limited to T = 250, 300, and 350 °C.

3.4.1. *Trap depth*

If we consider these subtracted TL curves to be the charge lost during specific hold-time ranges, then the shape of these curves should contain useful kinetic information. The initial rise portion of these subtracted TL curves was fitted in the same way as in Section 3.3 to determine the apparent thermal trap depth; hereafter, this will be called the post-isothermal TL (pI-TL) method. The results for the regenerative and natural signals are shown in Fig. 5(a) and (e), respectively.

Just as with the FGC E-values following a regenerative dose (Fig. 2(b)), these pI-TL E-values steadily increase as deeper thermal regions are probed (Fig. 5(a)). Apparent E-values increase from about 0.73 eV to a seeming plateau around 1.86 (K-feldspar sample J0165). It is notable that the lowest value is similar to the values from the IRM and the VHRM for the 64 Gy irradiation in Sections 3.1 and 3.2. Additionally, this upper limit is higher than the highest FGC E-value (1.5 eV) observed for this sample.

The pI-TL regenerative E-values were also measured for samples J0995 (high albite), J0999 (perthite), and J1001 (perthite). A mean value of $E = 1.84 \pm 0.06$ eV was calculated from the final three hold intervals (30 - 100, 100 - 300, and 300 - 1000 s) at 350 °C for the regenerative signals of all four feldspar samples. While samples J0165 and J0995 may plateau at these durations, samples J0999 and J1001 exhibited a positive slope, suggesting that the maximum E-value may be higher for these two samples. (That structurally well-ordered feldspars like perthites should have greater maximum stability than those which formed at higher temperatures and exhibit more uniform composition (e.g., Ab and Or) is consistent with the observation of Visocekas et al. (1994) that athermal fading rates increase with greater structural disorder.) The average plateau value for J0165 and J0995 is only 1.86 ± 0.03 eV. Whether this plateau is real or apparent requires further investigation.

The trap depths measured for the natural pI-TL signals are generally consistent with the regenerative signals at the same isothermal conditions. Because of low signal intensity, the final subtracted curve at 350 °C (300 - 1000 s) was unsuited for analysis. The next two longest durations at 350 °C, however, give E-values of 1.81 and 1.86 eV and are in good agreement with the plateau found after regenerative doses, lending further support to the idea of a maximum value near 1.86 eV.

3.4.2. *Kinetic order*

The shapes of the pI-TL curves (Figs. 3(b) and 4(b)-(d)) resemble what would be expected under mixed-order kinetics. This conjecture can be quantified with the TL curve symmetry factor of Halperin and Braner (1960), μ_g, which can be used to assign kinetic order to TL curves based on shape with little dependence on E or s values (Chen and Kirsh, 1981, pp. 159 - 167).

Calculated symmetry factors for the pI-TL curves (excluding the initial 0 - 3 s measurement) yield an average kinetic order of 1.6 ± 0.3 for the regenerative signals and 1.5 ± 0.5 for the natural signals (Fig. 5(d) and (h)). There is no apparent relationship between hold temperature and the kinetic order for most sets of hold temperatures. This relatively stable kinetic order with greater temperature is consistent with the interpretation that the pathways are unchanging, whereas the probed lifetimes increase with TL temperature.

The high b-values for the natural signals lost at 250 °C between 3 - 10, 10 - 30, and 30 - 100 s ($b = 2.2$, 2.3, and 2.1, respectively) may be an exception to this uniformity. That kinetic order is higher as the natural signal is initially depleted may be caused by charge transfer to sites of greater thermal stability.

3.4.3. Frequency factor

Finally, given that each pI-TL curve has an apparent trap depth and kinetic order, we can estimate the corresponding frequency factors. The calculation assumes general-order kinetics, and requires kinetic order (b), trap depth (E), temperature at maximum intensity (T_m), and heating rate (β) to determine the frequency factor (s) (p. 11; Chen and Kirsh, 1981):

$$s(b-1)/\beta \int_{T_0}^{T_m} \exp\Big(-E/k_B T\Big) dT + 1 = \Big(sbk_B T_m^2/\beta E\Big) \exp\Big(-E/k_B T_m\Big). \tag{3}$$

This calculation was performed under two different scenarios. In the first scenario, the E-value measured for each isothermal condition was used to calculated the corresponding frequency factor. In the second, the plateau value of 1.86 eV was used to calculate the apparent frequency factor for each pI-TL curve.

Assuming individual E-values. If each pI-TL curve derives from different trap depth (or range of depths), the frequency factors for the regenerative and natural signals are shown in Fig. 5(b) and (f). The regenerative values seem to increase with hold time, especially those at $T = 100$, 300, and 350 °C, but the results from the other hold temperatures are less convincing. This result is unexpected if this broad regenerative peak represents an increase in recombination-by-tunneling distances; this mechanism should produce the opposite effect: a decrease in the apparent frequency factor as sites increase in stability (Jain and Ankjaergaard, 2011; Jain et al., 2015).

While both natural and regenerative frequency factors span a similar range ($\sim 10^{11} - 10^{13}\ s^{-1}$), the former seem less organized. This may represent the lower signal intensities involved, resulting in poor fittings of E or b values. Alternately, the peak overlap from a higher temperature peak (e.g., Fig. 4 (b) - (d)) may sufficiently distort the T_m value or the position of T_2 ($T_{1/2} > T_m$).

Assuming a shared E-value of 1.86 eV. If each pI-TL curve derives from a single trap depth of 1.86 eV (see Section 3.4.1), the frequency factors for the regenerative and natural signals are shown in Fig. 5(c) and (g). The consistent decrease in apparent frequency factor with increasing hold time and temperature is consistent with the interpretation that K-feldspar thermoluminescence derives from a single dosimetric trap via tunneling to centers at a variety of distances (Jain and Ankjaergaard, 2011). Such an interpretation would result in a range of apparent frequency factors which reflects the range of recombination probabilities (Jain et al., 2015). We favor this simple interpretation (i.e., one trap depth of 1.86 eV, many apparent frequency factors).

Finally, it is remarkable that the frequency factors for the natural and regenerative signals decrease at a similar rate and over a similar range. Such similarity supports the conjecture that the natural signal for sample J0165 contains the stable portion of the signal measured after laboratory irradiation and exhibits similar kinetic properties.

4. Discussion

4.1. Comparing the methods for E-value determination

To interpret the results from these four methods, it is helpful to consider their critical assumptions. The initial rise method assumes that detrapping, at least for the first portion of the emitted peak, is related only to the ratio of E/k_BT (Eq. 1). In other words, effects like retrapping and changes in recombination efficiency should be negligible. The method also requires that the entire fitted region derives from the same trap and does not include overlapping peaks. With the IRM, a single E-value is produced that, for glow curves without overlapping emissions, corresponds to the first accessed trap. The various heating rates method also produces a single E-value and assumes that neither the trap depth nor the frequency factor change during the TL measurement. The fractional glow curve method incorporates the assumptions of the IRM but offers the possibility of measuring multiple trap depths, provided that each initial rise region is sufficiently separated for the chosen heating rate and stop-temperature increment.

The post-isothermal TL method is similar in approach to the FGC method: the TL curve is progressively measured, allowing for multiple E-value analyses. Unlike the FGC, however, the pI-TL method is not inaccurate if there is trap overlap initially, as the next measured curve is subtracted before analysis (in the case of no overlap, the pI-TL method would reduce to the FGC method for E-value determination). Another advantage obtained by considering the emissions between hold times is that peak shape analyses can be performed, including the evaluation of b and s values for each isothermal time range. Because feldspar TL is known to exhibit overlapping emissions, we consider the pI-TL results least subject to error.

4.2. Comparing the measured E-values

Notable concordance is found between the initial rise method and the various heating rates method. For the VHRM, the data seem to be sub-linear rather than linear as would normally be expected. This effect probably reflects the asymmetric nature of the feldspar TL glow curve: the initial rise region of the curve would be less affected, but in measuring the T_m value, the influence of overlapping, higher-stability traps biases the E-value determination. This effect should vary with heating rate, as lower heating rates will tend to minimize this trap separation effect. Importantly, the feldspar samples did not receive preheats prior to the measurement of apparent natural E-values.

The FGC E-values obtained compare well with experimental results reported elsewhere from sedimentary K-feldspars. Previous studies have reported values ranging from 0.4 eV at liquid nitrogen temperatures (Visocekas et al., 1996) to about 1.7 eV at temperatures above 280 °C (Strickertsson, 1985; Chruścińska, 2001). All of these studies also noted the linear increase in E with FGC hold temperature.

Several observations can be made about the regenerative E-values derived from the post-isothermal TL method. First, just as with the FGC, a linear relationship exists between the isothermal duration and the corresponding E-value. A similar type of analysis on a museum specimen of plagioclase was done by Pagonis et al. (2014), who performed a general-order kinetics fitting of TL curves gotten by subtraction of post-isothermal TL curves where hold temperatures were varied but not durations. These authors found a range of E-values from 1.1 to 1.8 eV, with a generally decreasing kinetic order, from about 2.0 to 1.5. Measurements for our albitic sample (J0995) are comparable, varying over a slightly broader range, from 0.76 to 1.87 eV (omitting the 0-3 s measurement, the range becomes 0.97 to 1.87 eV).

There exists a plateau in regenerative pI-TL E-values at 1.86 $\pm$ 0.03 eV (J0165 and J0995; 1.84 $\pm$ 0.06 eV for all four samples) for the three highest E-values observed in our pI-TL method. We tentatively interpret this as the depth of the ground state for the main dosimetric trap (see also Section 4.4). Whether this is a maximum within a distribution of depths or the true trap depth (i.e., activation progresses up through the band-tail states finally into the conduction band) is unclear.

Another consideration is the difference between the FGC and pI-TL methods in the final values obtained for regenerative E-values. Both techniques yield final values which might be interpreted as plateaus: 1.49 $\pm$ 0.03 eV (FGC, last four values of J0165) and 1.84 $\pm$ 0.03 eV (pI-TL, last three values of J0165). Perhaps the best explanation for this discrepancy is that the reason for each 'upper limit' is different. In the regenerative fractional glow curve method, the sample receives a single dose before all measurements are performed. It seems reasonable to assume that above 320 °C the source traps have been emptied and that further measurements are comprised mostly of thermal background emissions. The FGC upper limit may, in this interpretation, be understood as methodological, not directly characteristic of trap parameters. By comparison, the pI-TL method involves irradiation of the sample prior to each isothermal treatment, thereby replenishing the source traps. The upper limit for this technique is governed also by the low signal intensity relative to the thermal background, but this is true only after treatments of 350 °C lasting 300 and 1000 s, which probe higher regions of the glow curve than those reached by the FGC method. Of course, the upper limit of this technique may also be limited by instrumental resolution and not by the maximum trap depth that would contribute TL at these measurement conditions.

Finally, it is encouraging that both the natural and regenerative doses yield similar E-values for J0165 when evaluated with the pI-TL method. This is true for both the rising values measured at T = 250, 300, and 350 °C, and for the uppermost values: 1.86 $\pm$ 0.03 eV ($n = 3$) for the regenerative dose, and 1.84 $\pm$ 0.04 eV ($n = 2$) for the natural dose.

4.3. Kinetic order and frequency factor values

The pI-TL kinetic order values of 1.6 $\pm$ 0.3 for the regenerative signals and 1.5 $\pm$ 0.5 for the natural signals (Fig. 5(d) and (h)) compare well and show no obvious dependence on hold temperature. This may indicate that similar recombination pathways are utilized during the entirety of the TL measurement.

Assuming that a) the application of Eq. 3 to pI-TL curves is valid, and b) the TL emissions share an actual (i.e., not apparent) E-value of $\sim$1.86 eV, the apparent frequency factor decreases regularly over the entire range of hold temperatures and durations (Fig. 5(c) and (g)). Even more striking is the correspondence between the natural and regenerative pI-TL frequency factors. This correspondence lends credence to the hypothesis that the natural and regenerative TL glow curves may receive contributions from the same trap population, with the natural signal missing the nearer trap-and-center pairs, i.e., a truncated $n(r)$ distribution in Jain et al.'s (2015) model. That a shared E-value produces expected behavior in apparent frequency factors may favor the interpretation of a single trap depth responsible for the lower-temperature blue-green TL emissions (Jain et al., 2015) instead of a continuum of trap depths (Sanderson, 1988).

4.4. Relating the pI-TL E-value to IRSL signals

A primary concern when evaluating luminescence ages from K-feldspars is the thermal trap depth associated with the IRSL signal. Workers have investigated this parameter through the use of pulse-annealing experiments and the reduction of TL curves by IR stimulation (Li and Aitken, 1989; Duller and Wintle, 1991; Duller and Bøtter-Jensen, 1993; Duller, 1994; Tso et al., 1996; Murray et al., 2009). The interpretation of these experiments has not been straightforward, however, for although exposure to IR light depletes a broad region of the regenerative TL curve at lower temperatures, the majority of the IRSL source trap does not seem to be depleted significantly until higher temperatures. This reduction in TL intensity at lower measurement temperatures (i.e., the region populated after irradiation and without preheating) following IR exposure has been explained as a reduction in recombination efficiency (Murray et al., 2009). (If the loss of efficiency is related to the depletion of a shared recombination center, this explanation reconciles the similar emission spectra for K-feldspar TL and IRSL (Huntley et al., 1988, 1991).) More recently, Jain and Ankjaergaard (2011) have suggested that the lower- and higher-temperature TL peaks commonly found in feldspars may derive from a) localized recombination via the excited state of the trap, and b) recombination from the band-tail states (transitioning eventually into the conduction band), respectively. Under this interpretation, and given that the excited state is thought to lie within the band-tail states (Poolton et al., 2009), the uppermost pI-TL E-value should represent the thermal depth of the main dosimetric trap measured in IRSL protocols.

5. Conclusions

The similarity of pI-TL kinetic parameters between natural and artificial TL signals is intriguing and merits further exploration. The implication that the natural TL signal represents the high-stability region of a trap continuum may be overly simple, especially given previous studies which demonstrate differential thermo-optical bleaching properties between the low and high-temperature regions of the TL curve. Nevertheless, the agreement between the uppermost E-values of about 1.86 eV offer insight into the maximum thermal stability that may be expected for alkali feldspars extracted from bedrock samples. Finally, the temperature-independent kinetic order values combined with the decreasing apparent frequency factor values at higher temperatures and longer hold times both support the recent hypothesis that feldspar TL (in addition to IRSL) derives from distance-dependent tunneling recombination.

Acknowledgements

The authors would like to thank Natalia Somolatova, David Sammeth, and Andreas Lang for their help with sample collection. Tomas Capaldi and Natalia Somolatova are also thanked for preparing some of the samples for analysis. Rosario Esposito graciously assisted with electron probe analysis. This manuscript was greatly improved by the input from two anonymous reviewers.

References

Ankjaergaard, C., Murray, A.S., Denby, P.M., Bøtter-Jensen, L., 2006. Measurement of optically and thermally stimulated electron emission from natural minerals. Radiation Measurements 41, 780–786.

Balescu, S., Lamothe, M., 1992. The blue emission of K-feldspar coarse grains and its potential for overcoming TL age underestimation. Quaternary Science Reviews 11, 45–51.

Bøtter-Jensen, L., Andersen, C.E., Duller, G.A.T., Murray, A.S., 2003. Developments in radiation, stimulation and observation facilities in luminescence measurements. Radiation Measurements 37, 535–541.

Chen, R., 1969. Glow curves with general order kinetics. Journal of the Electrochemical Society: Solid State Science 116, 1254–1257.

Chen, R., Kirsh, Y., 1981. Analysis of thermally stimulated processes. Pergamon.

Chen, R., McKeever, S.W.S., 1997. Theory of thermoluminescence and related phenomena. World Scientific.

Chruścińska, A., 2001. The fractional glow technique as a tool of investigation of TL bleaching efficiency in K-feldspar. Geochronometria 20, 21–30.

Duller, G.A.T., 1994. A new method for the analysis of infrared stimulated luminescence data from potassium feldspars. Radiation Measurements 23, 281–285.

Duller, G.A.T., 1997. Behavioural studies of stimulated luminescence from feldspars. Radiation Measurements 27, 663–694.

Duller, G.A.T., Bøtter-Jensen, L., 1993. Luminescence from potassium feldspars stimulated by infrared and green light. Radiation Protection Dosimetry 47, 683–688.

Duller, G.A.T., Wintle, A.G., 1991. On infrared stimulated luminescence at elevated temperatures. Nuclear Tracks and Radiation Measurements 18, 379–384.

Grün, R., Packman, S.C., 1994. Observation on the kinetics involved in the TL glow curves in quartz, K-feldspar and Na-feldspar mineral separates of sediments and their significance for dating studies. Radiation Measurements 23, 317–322.

Guralnik, B., Jain, M., Herman, F., Ankjaergaard, C., Murray, A.S., Valla, P.G., Preusser, F., King, G.E., Chen, R., Lowick, S.E., Kook, M., Rhodes, E.J., 2015. OSL-thermochronometry of feldspar from the KTB borehole, Germany. Earth and Planetary Science Letters 423, 232 – 243.

Halperin, A., Braner, A.A., 1960. Evaluation of thermal activation energies from glow curves. Physical Review 117, 408 – 415.

Huntley, D.J., Godfrey-Smith, D.I., Haskell, E.H., 1991. Light-induced emission spectra from some quartz and feldspars. Nuclear Tracks and Radiation Measurements 18, 127–131.

Huntley, D.J., Godfrey-Smith, D.I., Thewalt, M.L.W., Berger, G.W., 1988. Thermoluminescence spectra of some mineral samples relevant to thermoluminescence dating. Journal of Luminescence 39, 123–136.

Huot, S., Lamothe, M., 2012. The implication of sodium-rich plagioclase minerals contaminating K-rich feldspar aliquots in luminescence dating. Quaternary Geochronology 10, 334–339.

Jain, M., Ankjaergaard, C., 2011. Towards a non-fading signal in feldspar: Insight into charge transport and tunnelling from time-resolved optically stimulated luminescence. Radiation Measurements 46, 292–309.

Jain, M., Guralnik, B., Andersen, M.T., 2012. Stimulated luminescence emission from localized recombination in randomly distributed defects. Journal of Physics: Condensed Matter 24, 385402.

Jain, M., Sohbati, R., Guralnik, B., Murray, A.S., Kook, M., Lapp, T., Prasad, A.K., Thomsen, K.J., Buylaert, J.P., 2015. Kinetics of infrared stimulated luminescence from feldspars. Radiation Measurements 81, 242–250.

Kirsh, Y., Shoval, S., Townsend, P., 1987. Kinetics and emission spectra of thermoluminescence in the feldspars albite and microcline. Physica Satus Solidi A 101, 253–262.

Li, B., Li, S.H., 2013. The effect of band-tail states on the thermal stability of the infrared stimulated luminescence K-feldspar. Journal of Luminescence 136, 5–10.

Li, S.H., Aitken, M.J., 1989. How far back can we go with the optical dating of k-feldspar, in: Long and short range limits in luminescence dating. Research Laboratory for Archaeology and the History of Art. Occasional Publication Number 9.

Li, S.H., Tso, M.W.W., Wong, N.W., 1997. Parameters of OSL traps determined with various heating rates. Radiation Measurements 27, 43–47.

Li, S.H., Tso, M.Y., 1997. Lifetime determination of OSL signals from potassium feldspar. Radiation Measurements 27, 119–121.

Murray, A.S., Buylaert, J.P., Thomsen, K.J., Jain, M., 2009. The effect of preheating on the IRSL signal from feldspar. Radiation Measurements 44, 554–559.

Pagonis, V., Morthekai, P., Kitis, G., 2014. Kinetic analysis of thermoluminescence glow curves in feldspar: evidence for a continuous distribution of energies. Geochronometria 41, 168–177.

Poolton, N.R.J., Bøtter-Jensen, L., Johnsen, O., 1995. Thermo-optical properties of optically stimulated luminescence in feldspars. Radiation Measurements 24, 531–534.

Poolton, N.R.J., Kars, R.H., Wallinga, J., Bos, A.J.J., 2009. Direct evidence for the participation of band-tails and excited-state tunnelling in the luminescence of irradiated feldspars. Journal of Physics: Condensed Matter 21, 485505.

Rhodes, E.J., 2015. Dating sediments using potassium feldspar single-grain IRSL: Initial methodological considerations. Quaternary International 362, 14–22.

Rudlof, G., Becherer, J., Glaefeke, H., 1978. Behaviour of the fractional glow technique with first-order detrapping processes, traps distributed in energy or frequency factor. Physica Status Solidi (a) 49, 121–124.

Sanderson, D.C.W., 1988. Fading of thermoluminescence in feldspars: characteristics an corrections. Nuclear Tracks and Radiation Measurments 14, 155–161.

Spotila, J.A., Farley, K.A., Sieh, K., 1998. Uplift and erosion of the San Bernardino Mountains associated with transpression along the San Andreas fault, California, as constrained by radiogenic helium thermochronometry. Tectonics 17, 360–378.

Strickertsson, K., 1985. The thermoluminescence of potassium feldspars–glow curve characteristics and initial rise measurements. Nuclear Tracks and Radiation Measurements 10, 613–617.

Tso, M.Y.W., Wong, N.W.L., Li, S.H., 1996. Determination of lifetime of infrared stimulated signals from potassium and sodium feldspars. Radiation Protection Dosimetry 66, 387–389.

Visocekas, R., Spooner, N.A., Zink, A., Blanc, P., 1994. Tunnel afterglow, fading and infrared emission in thermoluminescence of feldspars. Radiation Measurements 23, 377–385.

Visocekas, R., Tale, V., Zink, A., Spooner, N.A., Tale, I., 1996. Trap spectroscopy and TSL in feldspars. Radiation Protection Dosimetry 66, 391–394.

Wise, D.U., 2000. Laramide structures in basement and cover of the Beartooth uplift near Red Lodge, Montana. AAPG Bulletin 84, 360–375.

List of Figures

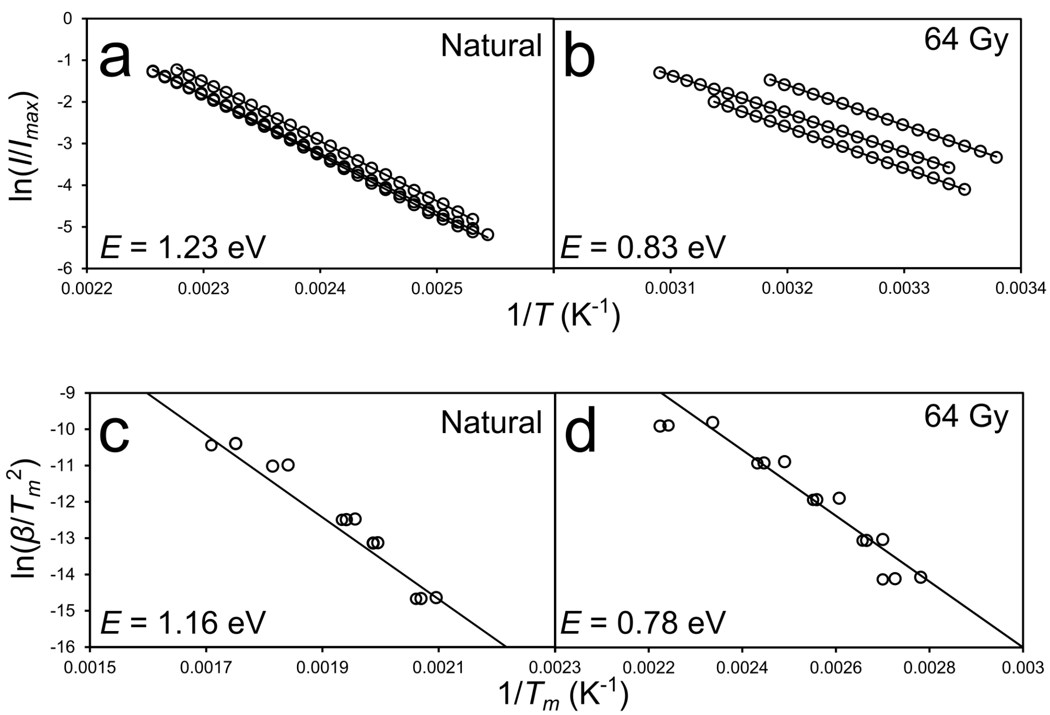

Figure 1: Apparent thermal trap depths for sample J0165 are calculated using the initial rise method (natural signal in (a) and regenerative signal after 64 Gy in (b)) and the various heating rates method (natural in (c) and 64 Gy in (d)). Note that the values calculated with the various heating rates method (1.16 and 0.78 eV) are slightly lower than those from the initial rise method (1.23 and 0.83 eV).

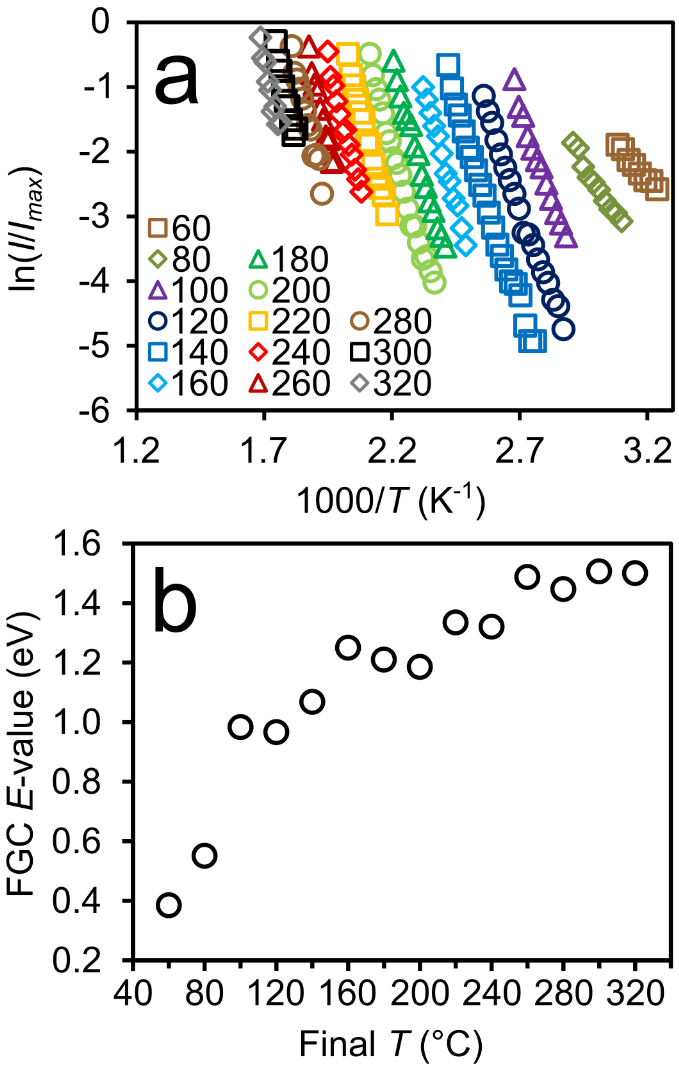

Figure 2: (a) Normalized thermoluminescence intensity plotted against inverse temperature for TL curves measured from $T =$ 60 to 320 °C in increments of 20 °C (sample J0165). (b) The data in (a) are fitted to calculate E-values for each of the TL curves within the fractional glow curve experiment.

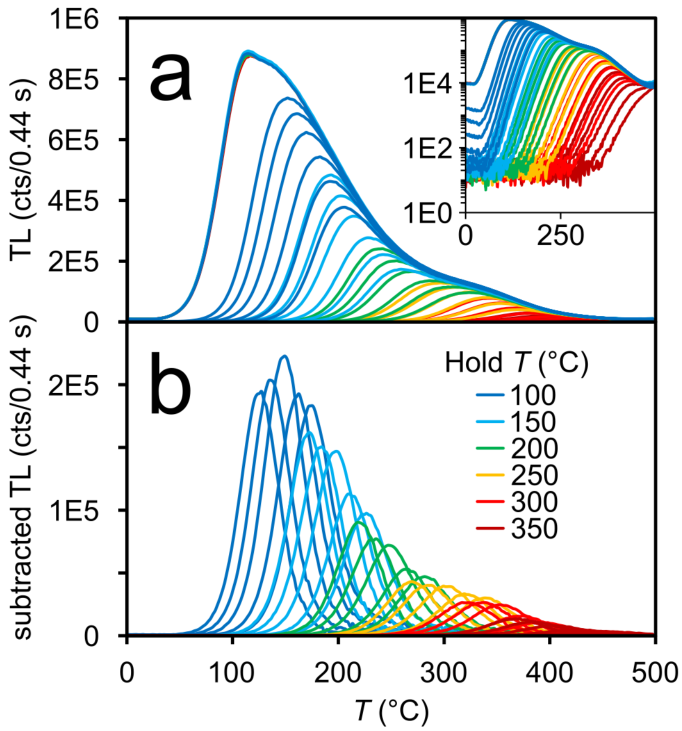

Figure 3: (a) Thermoluminescence curves for sample J0165 following irradiation and hold times t = 0, 3, 10, 30, 100, 300, and 1000 s at T = 100, 150, 200, 250, 300, and 350 °C. The same data are shown on a semi-log plot in the inset. (b) The loss between adjacent time steps (> 0 s) are plotted as subtracted TL glow curves. Notice how loss between hold times resembles mixed-order thermoluminescence.

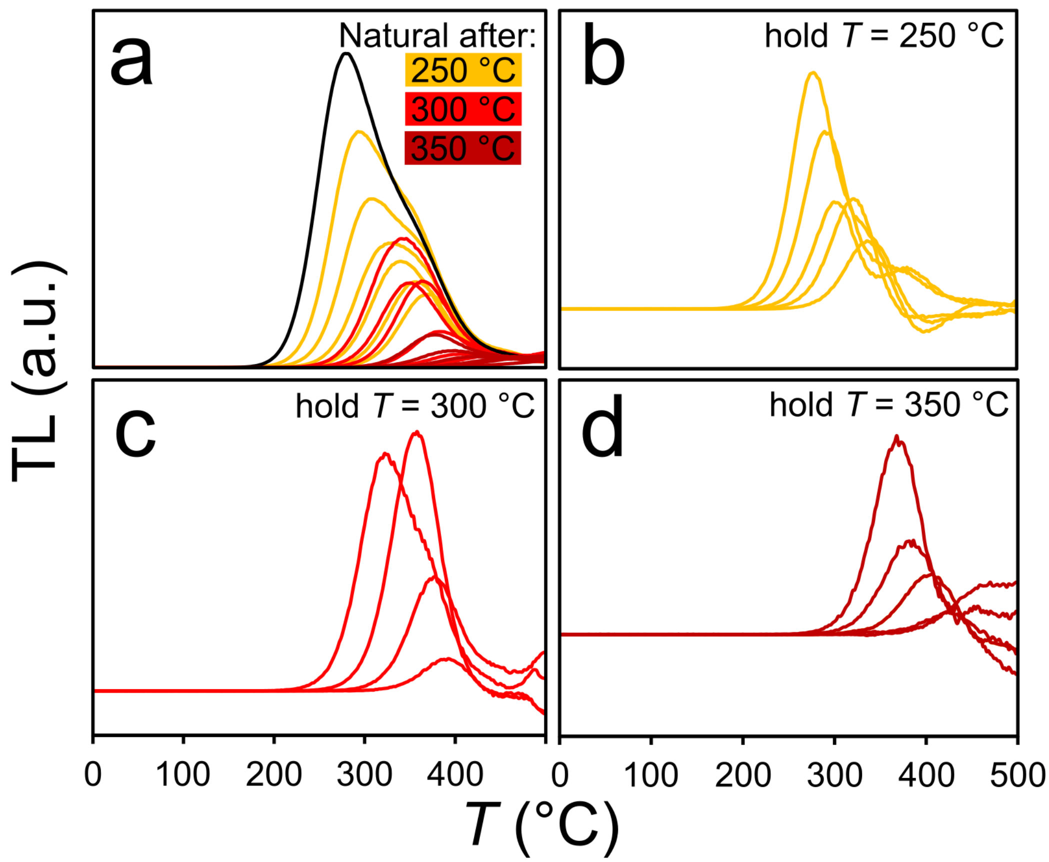

Figure 4: (a) The natural TL curve ($\beta = 5$ °C/s) is shown in black, as well as the natural curve following isothermal treatments $t = 3$, 10, 30, 100, 300, and 1000 s at $T = 250$, 300, and 350 °C (multiple aliquots of sample J0165). The natural TL curves are normalized to subsequent test-dose responses. The areas between the adjacent TL curves are shown for $T = 250$, 300, and 350 °C in (b),(c), and (d), respectively

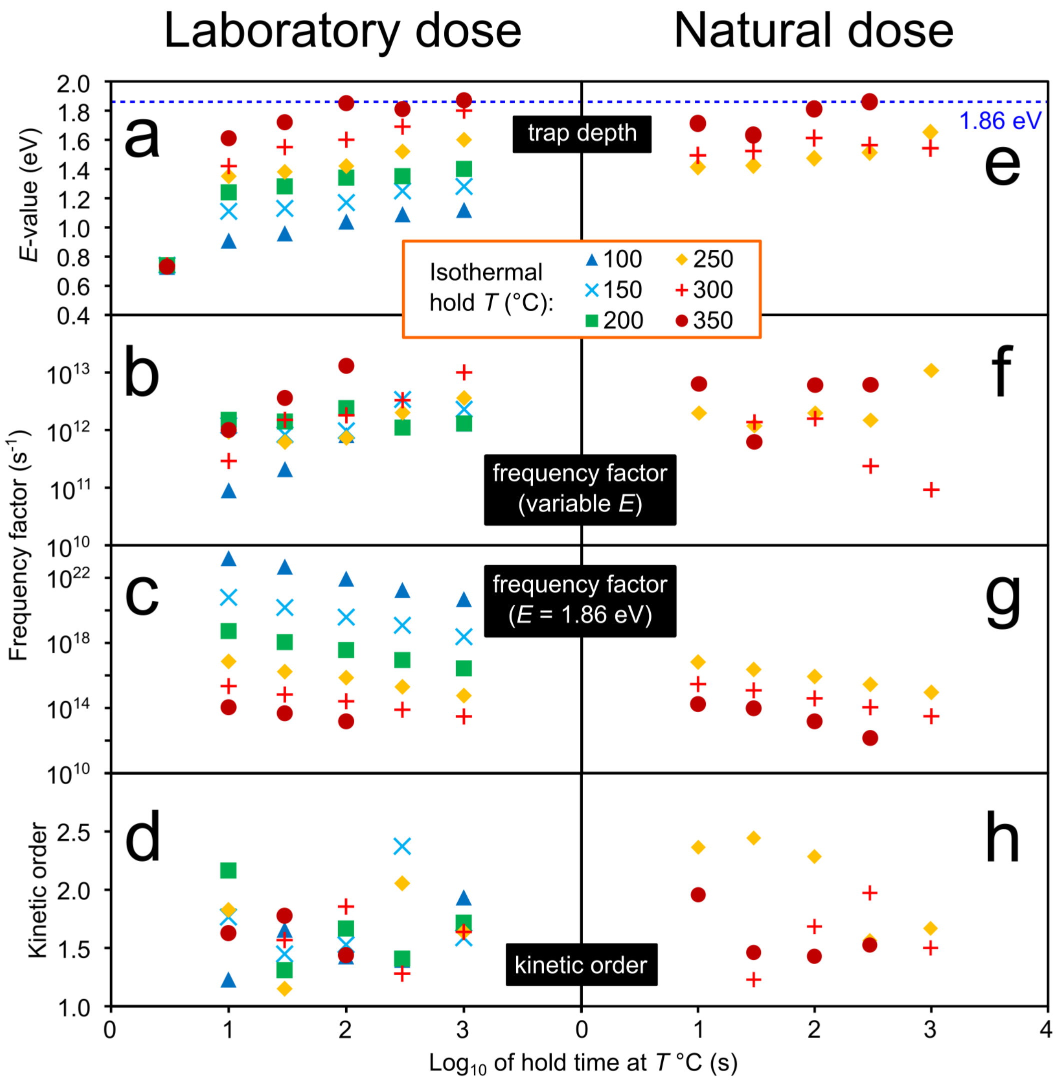

Figure 5: (a) Thermal trap depths of sample J0165 estimated for the regenerative signal using the pI-TL method (curves shown in Fig. 3(b)). Notice the correspondence with Fig. 2(b) and the apparent plateau around 1.86 eV. (b) Regenerative dose frequency factors are estimated assuming general-order kinetics, using the analytical expression for the temperature at maximum intesnsity, T_m (p. 11; Chen and Kirsh, 1981). (c) Identical to (b), except that the E-value is not calculated for each hold-time, but is instead set as 1.86 eV. This steady decrease in apparent frequency factor is consistent with the model for K-feldspar luminescence production wherein a trap of singular depth exhibits decreasing recombination probabilities as the tunneling distance increases (Jain and Ankjaergaard, 2011; Jain et al., 2015). (d) Kinetic order is estimated using the so-called geometrical factor, μ_g, a peak-shape parameter, following Chen (1969). The same parameters are shown in (e)-(h), following isothermal treatments of the natural signal. The hold temperatures for the natural signal are limited to 250, 300, and 350 °C.